Magnetic and Mössbauer-effect studies of U_6Fe hydride

H. Drulis

W. Trzebiatowski Institute of Low Temperature and Structure Research, Polish Academy of Sciences, P.O. Box 937,
50-950 Wrocław 2, Poland

F. G. Vagizov

Physicotechnical Institute, Russian Academy of Sciences, 420029, Kazan', Sibirskii Trakt 10/7, Russia

M. Drulis

W. Trzebiatowski Institute of Low Temperature and Structure Research, Polish Academy of Sciences, P.O. Box 937,
50-950 Wrocław 2, Poland

T. Mydlarz

International Laboratory of High Magnetic Fields and Low Temperatures, Gajowicka 95, 50-539 Wrocław, Poland

The dc magnetization, ac susceptibility, heat capacity, and Mössbauer effect for U_6FeH_{17} and β-UH_3 have been examined as a function of temperature (4.2–300 K) and magnetic field up to 140 kOe. The U_6FeH_{17} crystallizes in the $Pm3n$ space group where the metal arrangement is like that of β-W. The compound turned out to be a ferromagnet with a transition temperature of 173 K differing only slightly from that of β-UH_3. The saturation magnetization of U_6FeH_{17} at 140 kOe and at 4.2 K is smaller than that for β-UH_3. The temperature dependence of the ac susceptibility showed a sharp maximum of the χ' and χ'' at the para-ferromagnetic transition temperature for both investigated hydrides. In the U_6FeH_{17} hydride another steplike anomaly at about 140 K has been observed. This anomaly has been confirmed by heat capacity measurements. No such anomaly in β-UH_3 hydride has been reported for both mentioned above types of experiment. The valence-charge-density distribution and the main components of the electric field gradient tensor were calculated using the modified Thomas-Fermi approach. Mössbauer spectra analysis has shown that the iron atoms preferably occupy $(6c)$ sites in the U_6FeH_{17} lattice. It has been concluded that the [110] axis could be an easy magnetization direction in U_6FeH_{17} hydride.

I. INTRODUCTION

The absorption of hydrogen gas by the compounds of rare earth and actinide elements with $3d$ transition metals leads to substantial changes of their magnetic properties.[1] These include hydrogen-induced transitions from Pauli paramagnetism to ferromagnetism.[2] There are also examples of the reverse effect, i.e., where in the ferromagnetic compound the $3d$ moment disappears upon hydrogen absorption.[3] At first sight, no uniform behavior seems to exist regarding the changes in magnetic ordering temperatures accompanying the hydrogen absorption.

The changes in magnetic properties may have two different origins. In the first place, the introduction of hydrogen leads to the changes in the conduction electron concentrations, in the electron band filling, and in effective Coulomb repulsion. These effects, together with an increase of interatomic separation, can influence the exchange splitting of both the d and f electrons. The most spectacular example of hydrogen influence on the magnetic properties of actinide elements is UH_3 trihydride. Whereas α-uranium is a paramagnet with a rather weak temperature-dependent susceptibility, its hydride, β-UH_3, turns out to be a ferromagnet below $T_c = 178$ K.[4] The changes in magnetic properties were discussed in

Ref. 5 in terms of charge transfer and changes of interatomic distances. It was assumed that the magnetic properties of the hydride are due mainly to the localized $5f$ electrons which interact through the conduction electrons. Appearance of a narrow $5f$ band in the uranium hydride had been expected due to an increase of uranium interatomic distances above the Hill limit.[6] The hydrogen absorption in the actinide elements can also cause quite different modifications. In thorium metal, for example, it induces superconductivity.[7]

Such a correspondence is unusual and it would be interesting to investigate the hydrogen absorption effect on the physical properties of U_6Fe, one of the uranium high-field superconductors. It belongs to the group of the body-centered-tetragonal (bct) U_6M ($M =$ Mn, Fe, Co, Ni) type compounds. U_6Fe becomes a superconductor at 3.8 K.[8] The superconducting phase in the materials is characterized by rather small interatomic distances ($d_{U-U} = 300$ nm), falling below the Hill limit.[9] The magnetic measurements have shown that all the compounds are exchange-enhanced paramagnetics.[10–12]

To the best of our knowledge, of all mentioned compounds only U_6Co has been hydrogenated and its magnetic properties investigated.[13] Hydrogenation of U_6Co leads to U_6CoH_{18} compounds with the crystal structure

of the well-known UH_3 hydride and ferromagnetic transition temperature of $T_c = 185$ K.

Presently, we report the results of the structure, magnetization, heat capacity, and Mössbauer-effect measurements of U_6FeH_x hydride with $x = 17$. We also report the outcome of a magnetic properties study of the pure β-UH_3 trihydride which has been synthesized from the same uranium metal batch. These measurements have made the analysis of the results obtained for U_6Fe hydride easier.

II. EXPERIMENTAL DETAILS

Initial samples of U_6Fe were prepared by arc melting of pure elemental uranium and isotopically enriched (95%) ^{57}Fe metal in the inert argon atmosphere. To avoid the formation of UFe_2, a small excess of uranium was applied. After the arc melting the samples were homogenized by a low-temperature annealing as described elsewhere.[12]

The x-ray diffraction measurements made with Cu $K\alpha$ radiation showed that the samples were a single-phase material of bct U_6Mn type structure with the lattice parameters $a = 10.303$ Å and $c = 5.235$ Å. The powder samples of the hydride were obtained by heating lumps of the compound in hydrogen up to 300 °C at a pressure of 0.1 MPa. The composition was determined from the amount of H_2 taken up, measured volumetrically. The x-ray powder diffraction data were obtained using a Philips PW1050 diffractometer. The ac magnetic susceptibility measurements have been performed by the Lake Shore Model 7000 ac susceptometer. The heat capacity experiments were done with an adiabatic calorimeter in the temperature range from 4 to 255 K.

The Mössbauer measurements were carried out using a conventional constant acceleration spectrometer with ^{57}Co in chromium matrix. The velocity scale and isomer shift were calibrated relative to an α-Fe absorber at room temperature. The Oxford continuous-flow type cooling system was used to cool absorbers to low temperatures. Samples for Mössbauer experiments were mounted on an aluminum foil with BF6 varnish in an argon glove box before transferring the absorber into the vacuum shroud cryostat.

III. RESULT AND DISCUSSION

A. X-ray examination

The U_6Fe absorbs hydrogen up to the stoichiometry of U_6FeH_{17}. X-ray diffraction (XRD) patterns of the hydride can be indexed in terms of a simple cubic structure of β-UH_3 type with lattice parameter $a = 6.631$ Å. The XRD patterns were taken at room and liquid nitrogen temperatures. No essential changes of the lattice constant with temperature have been found.

Using the Rietveld profile analysis, the refinement of the atomic coordinates has been performed. The best fitting can be achieved for the space group $Pm3n$ in which a metal arrangement is like that of β-W: two metal atoms are at $(2e)$ sites (000), $(\frac{1}{2}\frac{1}{2}\frac{1}{2})$, whereas six other

metal atoms occupy the $(6c)$ positions $\pm(\frac{1}{2}0\frac{1}{4})$, $\pm(\frac{1}{2}\frac{1}{4}0)$, $\pm(0\frac{1}{2}\frac{1}{4})$. 24 hydrogen atoms per unit cell are arranged in $(24k)$ sites with two free position parameters: $y = 0.155$, $z = 0.303$. Unfortunately, in the limits of our experimental accuracy, the Rietveld analysis does not allow us to state what kind of crystallographic position is preferred by the iron atoms. Various superlattice models of the iron distribution have been considered, but they cannot be distinguished by means of the analysis.

We dedicated a lot of attention to examining the hypothetical tendency towards phase separation after U_6Fe hydriding. On the basis of our Mössbauer data and x-ray analysis we have discovered that the hydriding/dehydriding reaction at ambient temperature is fully reversible without any evidence for the sample degradation.

B. Magnetic studies

Magnetization-field data for the powdered samples of U_6FeH_{17} and UH_3 at 4.2 K are shown in Fig. 1. At 140 kOe the saturation magnetic moment per uranium atom is equal to $0.86(1)\mu_B$ for UH_3 and $0.79(1)\mu_B$ for U_6FeH_{17}. The measured saturation magnetization value for β-UH_3 is comparable to that given by Trzebiatowski, Sliwa, and Stalinski,[4] and Kaufman, Lin[14] and Henry.[15] Due to very large anisotropy of magnetic actinide compounds, the saturation moments obtained from magnetization measurements on powders are usually lower than the moments calculated from the neutron diffraction studies.[16,17] Therefore, we are going to discuss the difference in magnetization only. All independent magnetometric measurements shown in Figs. 1 and 2 indicated evidently (above experimental errors) that the magnetization in UH_3 is higher than for U_6Fe hydride.

The lower saturation magnetization in U_6FeH_{17} relative to UH_3 can be consistent with (1) an appearance of a relatively large magnetic moment on Fe atoms (about $0.42\mu_B$ per iron atom) and its antiparallel orientation to the U moment, (2) diminishing of uranium magnetic moment, or (3) a rotation of the spin direction from one major cubic axis to another one due to the change of magnetocrystalline anisotropy.

A change in the Fe moment upon the hydrogen absorption has been observed in many intermetallic compounds.[18] But in our case, as it results from the Mössbauer data (see Fig. 9), the average hyperfine field on iron nuclei appears to be too small to explain the observed magnetization differences. Therefore, the assumption that hydrogenation induces the large magnetic moment on the iron atom in U_6FeH_{17} must be rejected.

In Fig. 2 the temperature dependences of magnetization of U_6FeH_{17} and UH_3 in the field of 10 kOe are depicted. As is seen, the temperature dependences $(M\text{-}T)$ are similar for both samples, which indicates that in U_6FeH_{17}, as in UH_3, the dominant interaction is that between the U moments which determines the transition temperatures T_c of both hydrides. The suggestion about uranium moments diminishing in U_6FeH_{17} remains unproved, although it cannot be excluded.
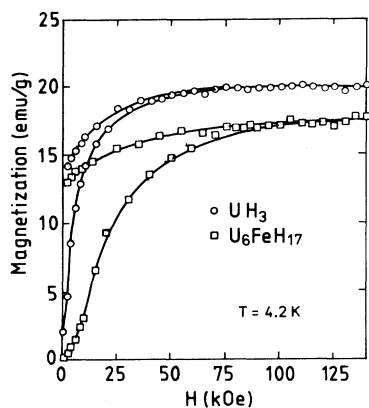
FIG. 1. Magnetization versus magnetic field at 4.2 K for U_6FeH_{17} and β-UH_3.

To verify the possibility of spin-reorientation transition (SRT) mentioned in (3), the ac susceptibility and the heat capacity measurements as a function of temperature were performed. Figure 3 shows the temperature dependence of the ac susceptibility of U_6FeH_{17} and UH_3 measured for powdered samples in zero dc external magnetic field. The sharp maxima on the real and imaginary parts of ac susceptibility at 176 and 183 K, respectively, in both investigated hydrides reflect the para-ferromagnetic transitions at these temperatures. At about 140 K another second steplike anomaly appears in the ac components of U_6FeH_{17}. There is no such anomaly for UH_3 samples. Unfortunately, this low-temperature anomaly has not been clearly observed when the ac magnetic susceptibility measurements were performed for randomly oriented powder samples.

C. Heat capacity measurements

To explain the origin of the low-temperature anomaly in the ac susceptibility, additional heat capacity measurements were performed. In Fig. 4 the molar specific heat
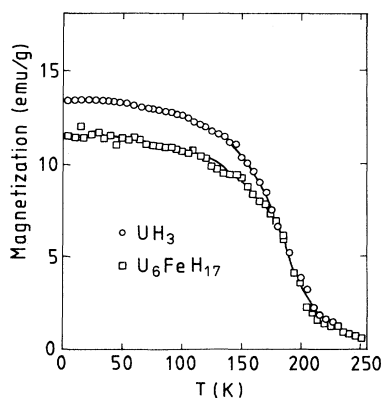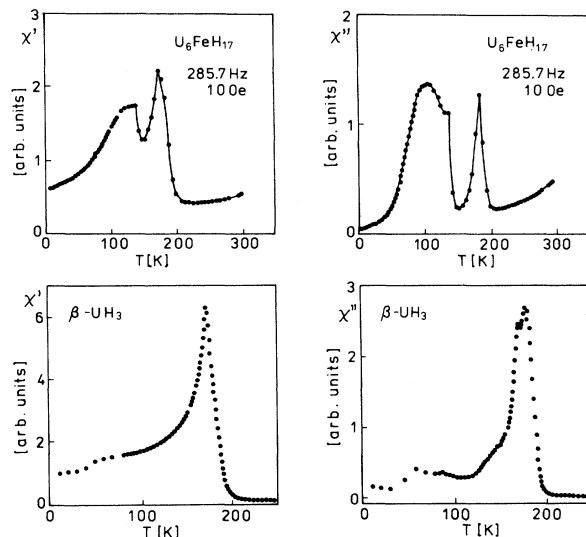

FIG. 3. The real χ' and imaginary χ'' parts of the ac susceptibility as measured in U_6FeH_{17} and UH_3.

as a function of the temperature is shown for U_6FeH_{17}. There are two anomalies in $C_p(T)$. The high-temperature anomaly at 173 K displays a para-ferromagnetic phase transition. The low-temperature anomaly has the behavior typical for the first-order type transition[19] and appears in the same temperature range where the ac susceptibility anomaly was registered. The specific heat data for UH_3 (Ref. 20) have not shown this type of anomaly.

We think that the low-temperature anomaly observed in the heat capacity experiments in U_6FeH_{17} should be ascribed to spin-reorientation transition. Since the Fe moment in U_6FeH_{17} is questionable, we think that the SRT could be successfully explained in terms of the competition between the electric field anisotropies of the two

FIG. 2. Magnetization vs temperature for U_6Fe hydride in 10 kOe magnetic field.
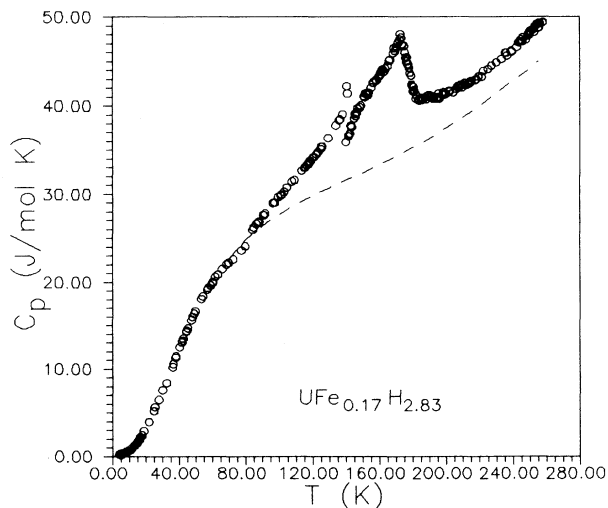

FIG. 4. The specific heat as a function of temperature of U_6Fe hydride sample. The dashed line represents the calculated electronic and lattice contributions.

noncrystallographically equivalent uranium sites. The change of the local environment of one of the uranium atoms, due to the iron presence in U$_6$FeH$_{17}$, can strongly act on the tendency to change an easy magnetization direction with temperature lowering. More information about the new magnetic state of U$_6$FeH$_{17}$ at low temperatures could be brought by neutron diffraction measurements.

D. ^{57}Fe Mössbauer-effect study

The ^{57}Fe Mössbauer spectra of the U$_6$Fe intermetallic compound measured at two different temperatures are shown in Fig. 5. The nuclear hyperfine structure parameters [isomer shift IS$=-0.34(3)$ mm/s and quadrupole splitting QS$=0.67(3)$ mm/s are in reasonable agreement with those reported previously in Refs. 21–23. Contrary to U$_6$Fe, quite different temperature dependence of Mössbauer spectra in U$_6$FeH$_{17}$ hydride is observed (compare Figs. 6 and 7). At low temperatures a strong broadening and complex structure of the spectra appear, which is associated with magnetic ordering. The complex structure can additionally be complicated by the fact that the iron atoms in U$_6$FeH$_{17}$ lattice might, in principle, occupy two nonequivalent crystallographic positions: (2e) and (6c).

For the (2e) site ($m\bar{3}$ symmetry) the nearest coordination sphere is formed by 12 equidistant hydrogen neighbors at an average distance 2.30 Å and by 12 uranium atoms at the distance 3.72 Å. The (6c) sites have point symmetry $\bar{4}m2$ with two neighbors at 3.31 Å and 12 hydrogen atoms at 2.30 Å. These two coordinations produce, of course, somewhat different charge-density distributions around the metal atoms.

To compare the electron density (ED) distribution around given sites in U$_6$FeH$_{17}$, we have performed the ED calculations using the modified statistic method of the Thomas-Fermi approach.[24] As in (Ref. 25), the simple form of pseudopotential has been used.
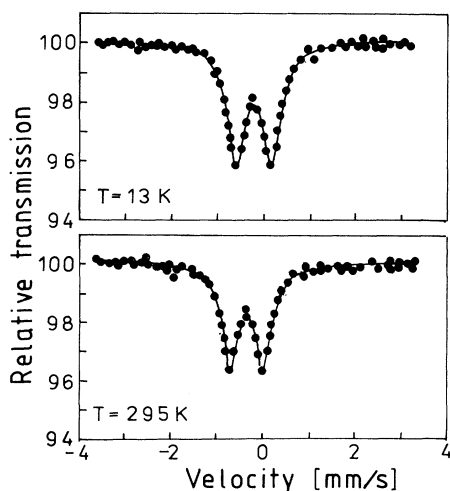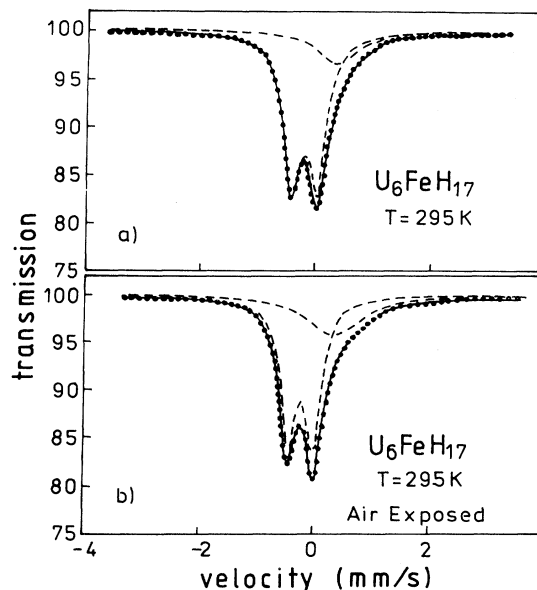

FIG. 6. The ^{57}Fe Mössbauer spectra of U$_6$FeH$_{17}$ before and after air exposure at room temperature.

FIG. 5. The ^{57}Fe Mössbauer spectra of the nonhydrogenated U$_6$Fe at 13 and 295 K.
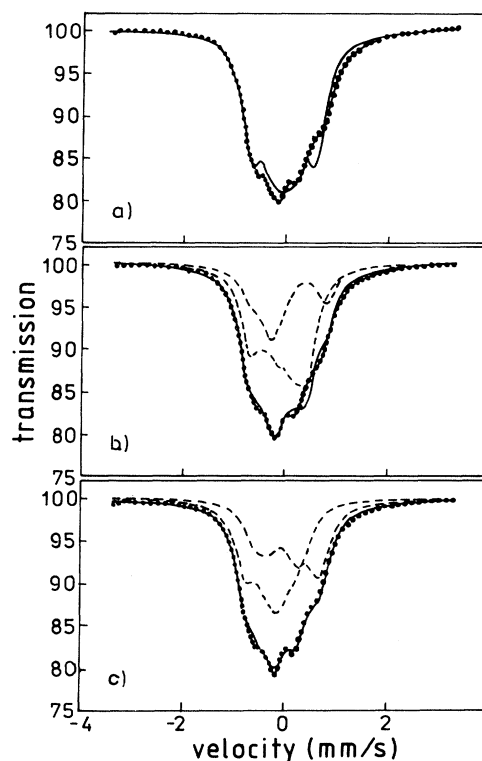

FIG. 7. The Mössbauer spectra of U$_6$FeH$_{17}$ at 13 K and the fitting analysis for (a) [111], (b) [100], and (c) [110] easy magnetization axes, respectively.

In Fig. 8 the valence-charge-density map in the plane of $z = \frac{1}{2}$ is shown. As one can see, the electron cloud around the (2e) $(\frac{1}{2}\frac{1}{2}\frac{1}{2})$ site is much more symmetric than that around the (6c) site. In Table I the calculated values of the main components of the electric field gradient (EFG) tensor for the obtained valence-charge distribution are shown. The direction coefficients of the EFG tensor are given in the last column. Table I reveals that if the iron atoms were statistically distributed among the (2e) and (6c) sites, the Mössbauer spectra of U_6Fe hydride in the paramagnetic state would consist of the quadrupole doublet and singlet with the area ratio of 3:1. However, as can be seen in Fig. 6, the experimentally found area ratio was close to 6:1. Moreover, one shall note that the isomer shift value for the singlet [IS$= +0.32(3)$ mm/s] is much larger than that for the doublet [IS$= -0.22(3)$ mm/s] and that for the initial U_6Fe [IS$= -0.34(3)$ mm/s]. The observed contradictions have inclined us to conclude that the singlet Mössbauer line probably does not belong to the U_6Fe hydride structure at all. This assumption has been confirmed by the line intensity increasing upon the exposure of the hydride sample to air [compare Figs. 6(a) and 6(b)]. All of these entitled us to state that the singlet belongs to an air-induced impurity and that the iron atoms preferably occupy the (6c) sites in U_6FeH_{17} only.

As it can be seen from Table I, the main axes of the EFG tensor are parallel to [100], [010], and [001] crystallographic axes, respectively. For crystals with cubic symmetry, the easy magnetization axes are directed, as a rule, either along the [111], [110], or [001] type axes. Since there is no access to the data on the easy magnetization axis for the studied hydride, the experimental spectra in Fig. 7 were fitted considering three different options:

(1) The easy magnetization direction in U_6FeH_{17} crystal is the [111] axis and thus the angles Θ between this direction and the EFG tensor components are the same for all (6c) sites and equal to $\Theta = 54.74°$. In such a case,
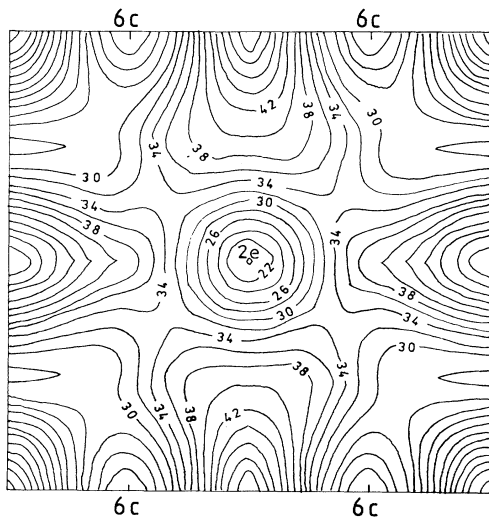
the Mössbauer spectra would consist of only one hyperfine pattern. This fitting is shown in Fig. 7(a).

(2) The easy magnetization axis is parallel to the crystallographic axis of [001] type and then, for $\frac{2}{3}$ of iron atoms, $\Theta = 90°$, whereas for the remaining ones, $\Theta = 0°$. In this option, the Mössbauer spectra should consist of two hyperfine components with the area ratio of 2:1. The best fit for this possibility is displayed in Fig. 7(b).

(3) The easy magnetization direction is set along the [110] axis. Now, the Mössbauer spectra should be also analyzed in terms of two six-line ^{57}Fe patterns with the area ratio of 2:1, but this time for the majority component the Θ should amount 45° and for the minority one, $\Theta = 90°$.

As one can see from Fig. 7(c), the last case seems to be the best fitting for the low-temperature Mössbauer spectra. For this χ^2 is almost three times smaller than in the

TABLE I. The main components of the EFG tensor, η, and directional cosines of EFG main components, calculated by the modified statistic method of the Thomas-Fermi approach.

Site	V_{zz}, V_{xx}, V_{yy} $\times 10^{-3}$ a.u.	$\eta = \dfrac{V_{xx} - V_{yy}}{V_{zz}}$	Orientation cosines of main axes of EFG tensor
$(\frac{1}{4}0\frac{1}{2})$	-10.59		1 0 0
	5.29	0.00	0 1 0
(6c)	5.29		0 0 1
$(\frac{1}{2}\frac{1}{4}0)$	-10.60		0 0 1
	5.30	0.00	1 0 0
(6c)	5.30		0 0 1
$(0\frac{1}{2}\frac{1}{4})$	-10.60		0 0 1
	5.30	0.00	1 0 0
(6c)	5.30		0 1 0
$(\frac{3}{4}0\frac{1}{2})$	-10.59		1 0 0
	5.29	0.00	0 1 0
(6c)	5.29		0 0 1
$(\frac{1}{4}0\frac{1}{2})$	-10.59		1 0 0
	5.29	0.00	0 1 0
(6c)	5.29		0 0 1
$(\frac{1}{2}\frac{3}{4}0)$	-10.60		0 1 0
	5.30	0.00	1 0 0
(6c)	5.30		0 0 1
$(0\frac{1}{2}\frac{3}{4})$	-10.60		0 0 1
	5.30	0.00	1 0 0
(6c)	5.30		0 1 0
(000)	-0.003		0 0 1
	0.000	1.00	1 0 0
(2e)	0.003		0 1 0
$(\frac{1}{2}\frac{1}{2}\frac{1}{2})$	-0.003		0 0 1
	0.000	1.00	1 0 0
(2e)	0.003		0 1 0

FIG. 8. The valence-charge-density distribution map in the plane of $z = \frac{1}{2}$ of U_6FeH_{17} unit cell.

previous cases. No improvement of the χ^2 value was observed taking into account all these three options simultaneously.

For all the cases, the fittings of experimental spectra were performed assuming that the linewidth and the isomer shift for both hyperfine components are the same. Both Mössbauer components differ from each other by Θ value only. As the free parameters, the following were chosen: magnetic hyperfine field H_{hf}, quadrupole splitting QS, and Θ—the angle between magnetic-field direction and the main axis (V_{zz}) of the EFG tensor. We also accepted an axial-symmetry model of the EFG with $\eta_1 = \eta_2 = 0$.

The fitting procedure for the low-temperature Mössbauer spectra in case (3) gives the following values: $H_{hf}^1 = 33.9$ kOe, $H_{hf}^2 = 14.9$ kOe; $QS_1 = 0.56(3)$ mm/s, $QS_2 = 0.66(3)$ mm/s; $\Theta_1 = 42.5(5)°$, $\Theta_2 = 93.1(5)°$. The obtained values of H_{hf} and QS for both components appeared to be somewhat different. This is unexpected in light of the fact that both the components originated from the Fe nuclei occupying probably the one type of crystallographic site only.

We think that the difference in the quadrupole splitting values and the small deviations of Θ from 45° and 90° indicated the possibility of small crystallographic deformations created by magnetostriction. In such a case, the crystallographic sites of Fe atoms, which are equivalent in the paramagnetic state, are no longer equivalent in the magnetically ordered state. In UFe_2,[26] for example, these interactions induce the orthorhombic deformation and the difference in the quadrupole splitting values can even reach the value of 0.25 mm/s; also the change of Θ in comparison to the ideal structure can be as large as 20°, up to 25°. In our case $\Delta QS = 0.10(3)$ mm/s, $\Delta\Theta_1 = -2.5(5)°$, $\Delta\Theta_2 = 3.1(5)°$. The observed difference between the hyperfine fields on iron atoms or U_6Fe hydride is very similar to that registered in UFe_2.[26,27] Its origin is mainly in the dipolar fields.

The temperature dependence of the average hyperfine field on Fe nuclei in U_6FeH_{17} is shown in Fig. 9. The solid line represents the approximation of the experimental data by the power function of $H_{hf} = H_0(1 - T/T_c)^\beta$ type, where $H_0 = 27$ kOe, $T_c = 180$ K, and $\beta = 0.38(2)$. The dashed line is a Brillouin type curve with $J = \frac{1}{2}$, $H_0 = 23$ kOe, and $T_c = 178$ K.

IV. CONCLUSION

The U_6Fe intermetallic compound forms a stable hydride phase of the β-UH_3 type structure with the lattice

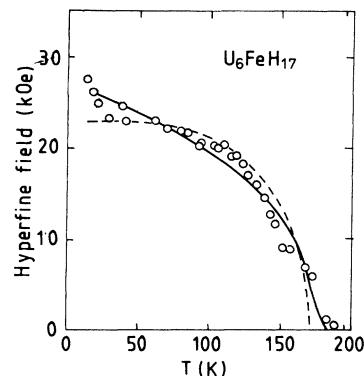
FIG. 9. Temperature dependence of the average hyperfine field, H_{hf}.

constant very close to that for the uranium hydride.

The magnetization measurements indicated that the magnetic behavior of the hydride was dominantly described by the uranium magnetic moments as in β-UH_3, but the saturation moment was smaller. This latter fact and the appearance of an additional anomaly on the $C_p(T)$ and the ac susceptibility versus temperature dependence revealed that the iron sublattice modifies the bulk magnetic properties of the hydride. The second anomaly in $C_p(T)$ at low temperatures seems to be related to the spin-reorientation transition.

The Mössbauer-effect analysis suggests that the [110] direction is probably an easy magnetization axis in the liquid helium temperature region and that the iron atoms preferably occupy (6c) sites in U_6FeH_{17}. The main contribution to the average hyperfine field measured on Fe nuclei comes apparently from the dipole interaction with the uranium moments. U_6FeH_{17} is the second uranium derivative hydride phase to be ferromagnetic and the first one with an evidence for spin-reorientation transition at lower temperatures. To confirm some of our conclusions, further investigation is planned (neutron diffraction).

[1]*Handbook of Magnetic Materials*, edited by K. H. J. Buschow (Elsevier, Amsterdam, 1991), Vol. 6, p. 511.

[2]K. H. J. Buschow, P. C. P. Bouten, and A. R. Miedema, Rep. Prog. Phys. **45**, 937–1039 (1982).

[3]K. H. J. Buschow and R. C. Sherwood, J. Appl. Phys. **49**, 1480 (1978).

[4]W. Trzebiatowski, A. Śliwa, and B. Staliński, Roczn. Chem.

26, 110 (1952); **28**, 12 (1954).

[5]A. C. Switendick, J. Less-Common. Met. **88**, 257 (1982).

[6]H. H. Hill, in *Plutonium and Other Actinides*, edited by W. N. Miner (The Metallogr. Soc. of the AIME, New York, 1970), Pt. 2.

[7]C. B. Satterthwaite and I. L. Toepke, Phys. Rev. Lett. **25**, 741 (1970).

[8]B. S. Chandrasekhar and J. K. Hulm, J. Phys. Chem. Solids 7, 259 (1958).

[9]H. H. Hill and B. T. Matthias, Phys. Rev. 168, 4649 (1968).

[10]F. Steglich, J. Aarts, C. D. Bredl, W. Lieke, D. Mescheda, W. Franz, and H. Schäfer, Phys. Rev. Lett. 43, 1892 (1979).

[11]H. R. Ott, H. Rudigier, Z. Fisk, and J. L. Smith, Phys. Rev. Lett. 50, 1595 (1983).

[12]L. E. DeLong, J. G. Huber, K. N. Yang, and M. B. Maple, Phys. Rev. Lett. 51, 312 (1983).

[13]A. V. Andreev, M. I. Bartashevich, A. V. Deryagin, L. Havela, and V. Sechovsky, Phys. Status Solidi A 98, K47 (1986).

[14]S. T. Lin and A. R. Kaufmann, Phys. Rev. 102, 640 (1956).

[15]W. E. Henry, Phys. Rev. 109, 1976 (1958).

[16]J. M. Fournier and L. Manes, in Structure and Bonding, edited by L. Manes (Springer-Verlag, Berlin, 1985), Vol. 59/60 pp. 127–196.

[17]A. C. Lawson, A. Severing, J. W. Ward, C. E. Olsen, J. A. Goldstone, and A. Williams, J. Less-Common. Met. 158, 267 (1990).

[18]K. H. J. Buschow, Solid State Commun. 19, 421 (1976).

[19]M. Drulis, J. Alloys Compounds 219, 41 (1995).

[20]J. J. Rush, H. E. Flotow, D. W. Connor, and C. L. Thaper, J. Chem. Phys. 45, 3817 (1966).

[21]S. Blow, J. Phys. Chem. Solids 30, 1549 (1969).

[22]C. W. Kimball, P. P. Vaishnava, A. E. Dwight, J. D. Jorgensen, and F. Y. Fradin, Phys. Rev. B 32, 4419 (1985).

[23]G. Lemon, P. Boolchand, M. Stevens, M. Marcuso, L. E. DeLong, and J. G. Huber, J. Less-Common. Met. 127, 329 (1987).

[24]I. M. Reznik, Fiz. Tverd. Tela 30, 3496 (1988) [Sov. Phys. Solid State 30, 2009 (1988)].

[25]M. L. Cohen, V. Heine, and D. Weaire, in Solid State Physics, edited by H. Ehrenreich, F. Seitz, and D. Turnbull (Academic, New York, 1970), Vol. 24, p. 480.

[26]V. D. Chechersky, V. V. Eremonko, and N. E. Kaner, Fiz. Nizk. Temp. 15, 191 (1989) [Sov. J. Low Temp. Phys. 15, 108 (1989)].

[27]J. Gal, Z. Hadari, E. R. Bauminger, I. Novik, S. Ofer, and M. Perkal, Phys. Lett. 31A, 511 (1970).